Mol Cell Biochem (2015) 410:111–120
DOI 10.1007/s11010-015-2543-7

Epigenetic regulation of human adipose-derived stem cells differentiation

Kristina Daniunaite[1] · Inga Serenaite[1] · Roberta Misgirdaite[1] · Juozas Gordevicius[2] · Ausra Unguryte[3] · Sandrine Fleury-Cappellesso[4,5] · Eiva Bernotiene[3] · Sonata Jarmalaite[1]

Received: 22 May 2015 / Accepted: 18 August 2015 / Published online: 26 August 2015

Abstract Adult stem cells have more restricted differentiation potential than embryonic stem cells (ESCs), but upon appropriate stimulation can differentiate into cells of different germ layers. Epigenetic factors, including DNA modifications, take a significant part in regulation of pluripotency and differentiation of ESCs. Less is known about the epigenetic regulation of these processes in adult stem cells. Gene expression profile and location of DNA modifications in adipose-derived stem cells (ADSCs) and their osteogenically differentiated lineages were analyzed using Agilent microarrays. Methylation-specific PCR and restriction-based quantitative PCR were applied for 5-methylcytosine (5mC) and 5-hydroxymethylcytosine (5hmC) detection in selected loci. The level of DNA modifications in the *POU5F1* locus was quantified with deep sequencing. Expression levels of selected genes were assayed by real-time PCR. ADSCs differentiation into osteogenic lineages involved marked changes in both 5mC and 5hmC profiles, but 5hmC changes were more abundant. 5mC losses and 5hmC gains were the main events observed during ADSCs differentiation, and were accompanied by increased expression of *TET1* ($P = 0.009$). In ADSCs, *POU5F1* was better expressed than *NANOG* or *SOX2* ($P \leq 0.001$). Both 5mC and 5hmC marks were present in the *POU5F1* locus, but only hydroxymethylation of specific cytosine showed significant effect on the gene expression. In summary, the data of our study suggest significant involvement of changes in 5hmC profile during the differentiation of human adult stem cells.

Keywords Adipose-derived stem cells · 5-hydroxymethylcytosine · *POU5F1*

Introduction

Human adipose tissue harbors a significant number of multipotent adult stem cells of mesenchymal origin known as adipose-derived stromal/stem cells (ADSCs). ADSCs can be induced to differentiate into mesodermal lineages (adipocytes, osteoblasts, myocytes, and chondrocytes), but upon certain conditions can differentiate into cells of other germ layers [1, 2]. Broad differentiation potential and convenient accessibility of ADSCs make them an attractive source of adult mesenchymal stem cells (MSCs) for regenerative medicine and cell developmental plasticity research.

Epigenetic mechanisms play a significant role in determination of developmental plasticity and cell fate specification. During cell differentiation, the pluripotency genes are epigenetically silenced, while the tissue-specific genes become differently activated in various tissues [3]. DNA

Electronic supplementary material The online version of this article (doi:10.1007/s11010-015-2543-7) contains supplementary material, which is available to authorized users.

✉ Sonata Jarmalaite
sonata.jarmalaite@gf.vu.lt

1 Division of Human Genome Research Centre, Faculty of Natural Sciences, Vilnius University, Ciurlionio 21, 03101 Vilnius, Lithuania

2 Institute of Mathematics and Informatics, Vilnius University, Akademijos 4, 08663 Vilnius, Lithuania

3 State Research Institute Center of Innovative Medicine, Zygimantu 9, 01120 Vilnius, Lithuania

4 EFS Pyreenees-Mediterranee, 31027 Toulouse, France

5 UMR5273 CNRS, EFS-INSERM U1031, Stromalab, 31432 Toulouse, France

methylation is a powerful mechanism of gene expression regulation. DNA methylation of promoter regions has been shown to silence gene expression, while the loss of methylation can restore transcription. Passive loss of DNA methylation can occur due to the reduced activity of DNA methyltransferases. In addition, the mechanism of active DNA demethylation was recently identified in embryonic stem cells (ESCs) [4, 5]. It was shown that TET enzymes catalyze oxidation of 5-methylcytosine (5mC) to 5-hydroxymethylcytosine (5hmC) and later derivatives, and in this way drive the process of DNA demethylation [4, 5]. Important role of Tet1 was identified in the maintenance of mouse ESC pluripotency through regulation of DNA methylation status of Nanog promoter [5]. Later it was shown that the silencing of Tet1 and Tet2 causes down-regulation of several pluripotency-related genes and premature differentiation of ESCs [6], suggesting significant involvement of 5hmC and TET enzymes in the maintenance of pluripotent state of ESCs. Moreover, recent studies reported dynamic redistribution of 5hmC marks [7, 8] during ESCs differentiation, indicating important role of this product of DNA demethylation in formation of gene expression pattern of differentiated cells. In comparison to ESCs, much less is known about the epigenetic profile of adult stem cells, including the distribution of 5hmC marks and the status of TET enzymes.

Differentiation potential of ESCs is regulated by the network of genes coordinated by key transcription factors POU5F1, NANOG, and SOX2. MSCs show lower expression of pluripotency genes [9] and more restricted differentiation potential than ESCs. However, similarly to ESCs, POU5F1, and NANOG are involved in regulation of developmental plasticity of MSCs [10, 11], and the list of POU5F1-regulated genes in MSCs is quite similar to that in ESCs [11]. Recent studies [12, 13] showed that differentiation potential of MSCs can be improved by DNA demethylating agents. ADSCs exposure to demethylating agent 5-azacytidine increased production of main pluripotency genes and improved differentiation spectrum of the cells, enabling generation of hepatocyte-like cells [12]. Moreover, occurrence of active demethylation during osteogenic differentiation of mouse ADSCs has been suggested [14], although no further investigations were done in this field.

For better characterization of epigenetic mechanisms occurring during differentiation of MSCs, gene expression profile and epigenetic DNA modifications (5mC and 5hmC) were analyzed in human ADSCs and their differentiated counterparts by genome-wide and locus-specific approaches. Expression levels of key epigenetic regulators *TET1*, *TET2*, and *EZH2*, and main pluripotency genes *POU5F1*, *NANOG*, and *SOX2* were also analyzed.

Methods

Cell cultivation and in vitro differentiation

Four ADSC lines were derived from plastic surgery residual material of three anonymous middle-aged healthy donors. Adipose tissues were collected at two study centers (Vilnius, Lithuania and Toulouse, France) according to the protocols approved by the Bioethics Committee in Lithuania (No. 6B-10-22) and by the Ministry of Education and Research in France (No. DC-2008-515). Informed consent was obtained from all individual participants included in the study.

Isolation and initial cultivation of ADSCs were performed according to standard protocols, established at the both study centers [15, 16], while further steps of cell cultivation and differentiation were performed according to the unified protocol as reported previously [16]. Briefly, cells were transferred to DMEM, supplemented with 10 % FCS and antibiotics, cultured in a humidified atmosphere with 5 % CO_2 at 37 °C, and passaged at subconfluence of 75–90 %. For characterization of MSC phenotype, cells were subjected for the cell surface marker analysis as previously described [15]. All cultured cells showed typical immunophenotype for ADSCs: the cells were positive for CD73, CD90, and CD105 surface markers, expressed low levels of CD34, and were negative for hematopoietic markers CD14 and CD45. Multilineage differentiation potential of ADSCs was confirmed through the induction of differentiation into osteogenic, adipogenic, and chondrogenic lineages at third passage according to standard protocols [16].

For genetic analyses, only cells of osteogenic differentiation were used together with their undifferentiated counterparts. ADSCs of the third passage were osteogenically induced by seeding at density $5 \times 10^3/cm^2$ and culturing in DMEM with 4.5 g/L glucose, containing 10 % FCS, 1 % antibiotics, 1×10^{-7} M dexamethasone, and 50 μg/mL ascorbic acid, for 21 days. Osteogenic differentiation was evaluated by staining with alizarin red S (Fig. 1a, b) according to standard protocols and additionally controlled by gene (*RUNX2* and *ALPL*) expression analysis.

RNA extraction

Total RNA was extracted from 2×10^6 cells on average with mirVana Kit according to manufacturer's protocol (Life Technologies, Forster City, CA, USA). RNA integrity number (RIN) was ≥9.4, as measured with 2100 Bioanalyzer system using RNA 6000 Nano Kit (Agilent Technologies, Santa Clara, CA, USA).

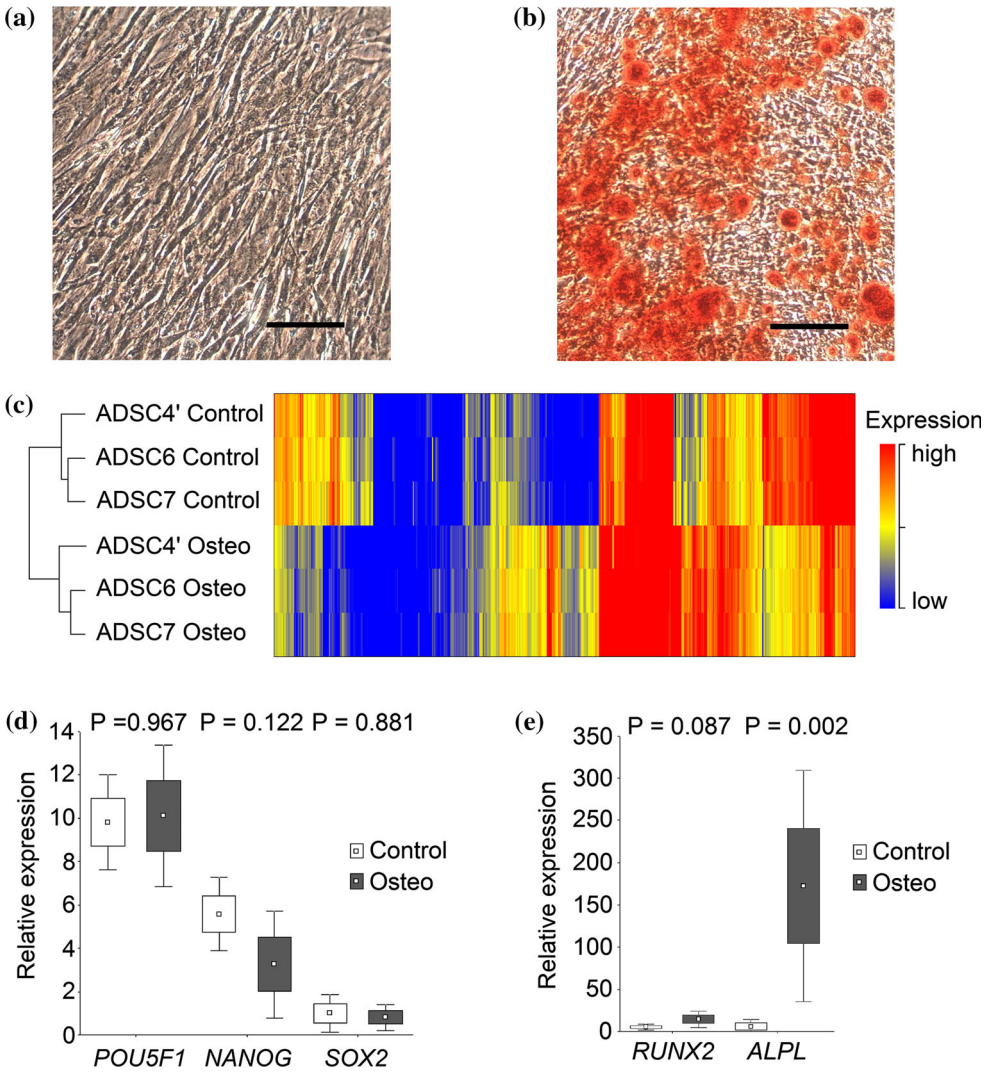

Fig. 1 Characterization of adipose-derived stem cells (ADSCs). Undifferentiated (**a**) and differentiated into osteogenic lineage (**b**) ADSCs stained with alizarin red S. **c** profile of genes that were significantly deregulated ($N = 455$) during osteogenic differentiation of ADSCs obtained by microarray analysis. Relative expression of pluripotency genes (**d**) and osteoblastic differentiation markers (**e**) in undifferentiated (Control) and osteogenically induced (Osteo) ADSCs was evaluated by means of RT-qPCR. Bars in photos indicate 100 μm

Global gene expression profiling

For global gene expression profiling, three pairs (undifferentiated and osteogenically induced) of ADSC lines from three donors were used. Microarray hybridization was performed according to manufacturer's protocol for One-Color Microarray-Based Gene Expression Analysis v6.5 (Agilent Technologies). Briefly, 200 ng of total RNA was labeled and amplified with Low Input Quick Amp Labeling Kit, One-Color and using RNA Spike-In Kit, One-Color (Agilent Technologies). After purification with RNeasy Mini Kit (Qiagen, Valencia, CA, USA), samples were hybridized onto Human Gene Expression (v2) 8 × 60 K microarrays, design ID 039494 (Agilent Technologies), for 17 h at 65 °C. Microarrays were scanned using SureScan microarray scanner and images were analyzed with Feature Extraction software v10.7 (Agilent Technologies). Data have been submitted to Gene Expression Omnibus repository, record number GSE63754 [17].

Target gene expression profiling by RT-qPCR

For cDNA synthesis, High Capacity cDNA Reverse Transcription Kit with RNase Inhibitor was used according to manufacturer's protocol (Life Technologies). Expression levels of selected genes—*POU5F1*, *NANOG*, *SOX2*, *TET1*, *TET2*, *EZH2*, *RUNX2*, *ALPL*, and endogenous control *EEF1A1*—were evaluated in all 4 pairs of cell lines using TaqMan Gene Expression Assays (Hs_00999632_g1, Hs_04260366_g1, Hs_04260357_g1, Hs_00286756_m1, Hs_00325999_m1, Hs_00544833_m1, Hs_00231692_m1, Hs_01029144_m1, and Hs_00265885_g1, respectively) by reverse transcription qPCR (RT-qPCR) in triplicates according to manufacturer's protocol (Life Technologies).

DNA extraction

Genomic DNA was extracted by digestion with proteinase-K followed by standard phenol/chloroform purification and ethanol precipitation. At least 1×10^6 of cells were used for DNA extraction.

MeDIP-chip and hMeDIP-chip

Methylated and hydroxymethylated DNA immunoprecipitation and microarray hybridization (MeDIP-Chip and hMeDIP-Chip, respectively) were performed following the guidelines of Agilent Microarray Analysis of Methylated DNA Immunoprecipitation v2.1 (Agilent Technologies). Briefly, 5 μg of DNA from three pairs of ADSCs used in gene expression profiling was sonicated with Bioruptor (Diagenode, Liege, Belgium) to fragments of 150–900 bp in size. One-fifth of sheared DNA was immunoprecipitated using 50 μL of Dynabeads Pan Mouse IgG (Life Technologies) and 5 μg of 5mC or 5hmC monoclonal antibody (Diagenode). DNA was then purified with phenol/chloroform using MaXtract High Density gel-filled tubes (Qiagen) and labeled using SureTag DNA Labeling Kit (Agilent Technologies). Cy5- and Cy3-labeled immunoprecipitated and reference samples were combined in a single mixture and hybridized onto Human CpG Island 244 K microarrays, design ID 014791 (Agilent Technologies), for 40 h at 67 °C.

Microarray data analysis

All microarray datasets were normalized using the same procedure starting from the raw data. Individual probe signals marked as saturated, non-uniform, or outlier were marked NA. Probes having an NA within at least one sample were removed from the analysis. The raw signal was log2 transformed and quantile normalized. Next, person effect was removed using residuals from a probe-wise linear model fit. Probe annotations were extracted from eArray platform [https://earray.chem.agilent.com] according to corresponding microarray design identifier. Promoter region was defined as ±500 bp around transcription start site, while the probes located downstream this point were assigned to intragenic region. Random annotations of (h)MeDIP-chip probes that showed significant differences between groups were checked manually. For each probe, *T* test was applied to compare two groups. Resulting *p* values were corrected for multiple testing using false discovery rate (FDR).

Locus-specific 5mC analysis

Four pairs of ADSC lines were involved in locus-specific 5mC analysis. Genomic DNA (400 ng) was exposed to bisulfite modification using EZ DNA Methylation kit (Zymo Research, Irvine, CA). Methylation-specific PCR (MSP) was used for the analysis of the methylation pattern in the regulatory 5′ regions of selected genes. The pairs of primers were designed using Methyl Primer Express v1.0 software (Life Technologies) or selected from publications (Online Resource 1). MSP assays were carried out in a reaction volume of 25 μL, consisting of 1 μL of bisulfite-modified DNA, 1 μM of each primer, and components of Maxima Hot Start Taq DNA polymerase kit (Thermo Fisher Scientific Baltics, Vilnius, Lithuania). The details of thermocycling are provided in Online Resource 1. Bisulfite-modified DNA from human brain (Zymo Research), as well as leukocytes of healthy donors, was used as the wild-type control. In vitro methylated leukocyte DNA (CpG methylase, Zymo Research) was used as a methylated control. Non-template (water) controls were always included in MSP.

Locus-specific 5hmC analysis

DNA from the same four cell lines involved in MSP analysis was also used for 5hmC quantification with Epi-JET 5-hmC Analysis Kit according to manufacturer's protocol (Thermo Fisher Scientific Baltics). The analysis involved DNA glucosylation and subsequent treatment with MspI, which digests genomic DNA when C, 5mC, or 5hmC is present within its recognition site (C↓CGG), but its activity is blocked when 5hmC is glucosylated (5ghmC). Products were then analyzed by qPCR with primers flanking particular MspI recognition sites. For each gene, two CCGG sites were analyzed: one located within 5′ regulatory region (promoter) and another in intragenic region (Online Resource 1).

5hmC-specific qPCR (5hmC-qPCR) was carried out on Mx3005P system (Agilent Technologies) in a reaction volume of 20 μL consisting of 1× Maxima SYBR Green qPCR Master Mix (2×), 10 nM of ROX (Thermo Fisher Scientific Baltics), 300 nM of each primer, and 10 ng of treated DNA. Each sample was run in duplicate and multiple non-template controls were included in each assay. The level of 5hmC (%), as compared to the total *C*, at a particular CpG was calculated based on $2^{-\Delta Cq}$ method ($\Delta C_q = C_qX - C_qN$, where *X* is the analyzed sample exposed to glucosylation and digestion, and *N* is the same sample not exposed to the enzymes). The reactions showing ΔC_q values lower than three cycles were not included into further calculations. Non-glucosylated but digested product was also used to control the difference between MspI exposed and nonexposed products. The specificity of amplification was always controlled by melting curve analysis.

BS-seq and TAB-seq

For quantitative evaluation of 5mC and 5hmC levels in the *POU5F1* locus, high throughput sequencing was used. Bisulfite sequencing (BS-seq) was applied to estimate the sum of 5mC and 5hmC levels, whereas TET-assisted bisulfite sequencing (TAB-seq) was used to distinguish 5hmC at a single-base resolution. For TAB-seq, 2 μg of genomic DNA was sonicated and further processed using 5hmC TAB-seq kit (Wisegene, Chicago, IL, USA). For BS-seq, DNA was treated with bisulfite as described above (Zymo Research).

Fusion primers, used to generate amplicon libraries for BS-seq and TAB-seq, were designed with IDT 454 Fusion Primers online tool (Integrated DNA Technologies, Coralville, IA, USA). PCR was performed using high fidelity Phusion U Hot Start DNA Polymerase (Thermo Fisher Scientific Baltics) in a 25 μL reaction volume containing: 1 × Phusion GC buffer, 500 nM fusion primers, 30 ng DNA, 200 μM of each dNTP, and 0.5 U of Phusion U Hot Start DNA polymerase. Amplification was performed as follows: 30 s at 98 °C, followed by 35 cycles of 10 s at 98 °C, 20 s at 62 °C, and 30 s at 72 °C; and 5 min at 72 °C. PCR products were analyzed with QIAxcel capillary electrophoresis system (Qiagen, Valencia, CA, USA) and further purified with Agencourt AMPure XP beads (Beckman Coulter, Barcelona, Spain). Amplicons were quantified fluorometrically using the Quant-iT PicoGreen dsDNA Assay kit (Life Technologies) and equimolarly pooled to create the multiplexed TAB-seq and BS-seq libraries at 1×10^6 molecules/μL. Emulsion PCR of each combined library was carried out using the GS Junior Titanium emPCR Kit (Lib-A) and sequenced onto a Titanium PicoTiterPlate (PTP) with Titanium reagents on the GS Junior 454 platform (all from Roche). The amplicons were sequenced bidirectionally with the average coverage of 2395×.

Results

Gene expression profile of ADSCs

Microarray-based gene expression profiling identified 455 unique genes that were significantly ($P < 0.05$) deregulated during osteogenic differentiation of ADSCs with fold change ≥1.5, of which 229 were up- and 226 down-regulated (Fig. 1c). Functional annotation analysis indicated that both up- and down-regulated genes were significantly ($P < 0.05$) represented by gene ontology (GO) terms like regulation of signaling and regulation of response to stimulus (Online Resource 2). Overexpressed genes were significantly involved in regulation of ossification and bone mineralization (e.g. *AXIN2*, *PTGER4*, *ADRB2*, and *P2RX7*). An indicator of osteogenesis alkaline phosphatase (*ALPL*) was also significantly up-regulated during osteogenic differentiation as well as genes encoding components of extracellular matrix, including laminins and collagens.

For additional characterization of ADSCs, the expression level of the key pluripotency genes *POU5F1, NANOG*, and *SOX2* was evaluated. The cells were characterized by a relatively high expression of the *POU5F1* transcript as compared to *NANOG* (2.25×, $P = 0.001$) or *SOX2* (11.0×, $P < 0.001$). Similar expression pattern remained after induced differentiation, and only *NANOG* showed 1.5× reduction ($P = 0.122$) of expression (Fig. 1d). Besides, osteogenically induced ADSCs showed marked upregulation of the main regulators of osteogenesis—*ALPL* (48.0×, $P = 0.002$) and *RUNX2* (2.8×, $P = 0.087$; Fig. 1e).

Epigenetic profile of ADSCs

To elucidate the extent of epigenetic changes during ADSCs differentiation, genome-wide methylation and hydroxymethylation analyses were performed. Global 5mC profiling identified significant ≥1.5-fold change of 5mC level in 394 genes, of which 130 genes were hypermethylated, while 267 were hypomethylated (including three redundant genes; Fig. 2a, b). More numerous changes occurred in the 5hmC profile (2.6× of 5mC changes), and the latter mark varied ≥1.5-fold in 1032 genes with the significant increase identified in 627 genes and reduction in 414 genes (including 9 redundant genes). Significant variation of the 5mC and 5hmC level was also observed in intergenic regions ($N = 126$ and $N = 309$ events, respectively; Fig. 2a). GO analysis showed that genes with 5mC and 5hmC changes were significantly ($P < 0.05$) represented by terms like cell fate commitment and regulation of transcription (Online Resource 2).

Of 394 genes with significant changes of the 5mC level, 212 genes showed 5mC variation in promoter region and 186 genes—in intragenic, with overlap of 4 genes between the two groups (Fig. 2b). Changes in the 5hmC level occurred in 579 gene promoters and 471 intragenic regions, including 18 redundant genes (Fig. 2b). 5hmC losses and 5mC gains were the most abundant events occurring during cellular differentiation and similar pattern of the changes was observed in all genic regions (Fig. 2b).

In order to correlate these frequent 5hmC changes with the presence of *TET* transcripts, *TET1* and *TET2* expression was assessed. Relatively low levels of both transcripts were detected in ADSCs, but significant upregulation ($P = 0.009$) of the *TET1* transcript was observed during the osteogenic differentiation (Fig. 2c). In addition, expression of the histone methyltransferase *EZH2*, usually

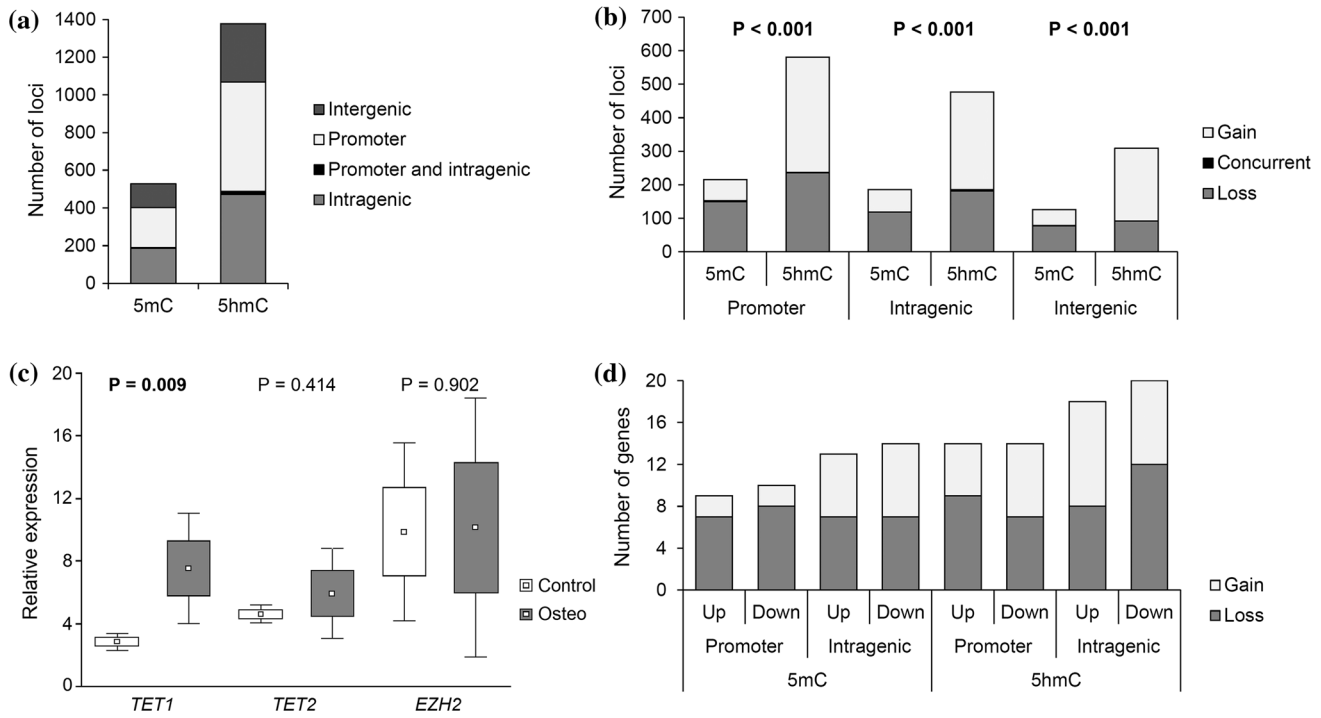

Fig. 2 Changes of epigenetic marks during adipose-derived stem cell differentiation into osteogenic lineage. **a** total 5mC and 5hmC changes according to genomic regions. **b** gains and losses of 5mC and 5hmC in different genomic regions. **c** relative expression of epigenetic regulator genes in undifferentiated (Control) and osteogenically induced (Osteo) ADSCs obtained by means of RT-qPCR. **d** association of significant epigenetic alterations with gene upregulation (*Up*) or down-regulation (*Down*). Data of 5mC and 5hmC changes were acquired with microarrays

up-regulated in stem cells, was analyzed for comparison and showed equally high expression both in undifferentiated and differentiated ADSCs.

5mC/5hmC marks and gene expression

For further evaluation of regulatory role of cytosine modifications, associations with gene expression were analyzed using less stringent threshold with fold change lowered to 1.2 for cytosine modifications data. Among the genes deregulated ($N = 455$) during the osteogenic differentiation of ADSCs, 82 had alterations of epigenetic marks (5mC and/or 5hmC) in promoter and/or intragenic regions, including 21 genes that had alterations of both marks.

Of these 82 genes, 41 were up- and 41 down-regulated. The loss of 5mC in promoter region (15 genes) was observed among both up- and down-regulated genes; however, deregulated gene expression was more specifically marked by changes in intragenic levels of 5hmC (35 genes; Online Resource 3). The gain of 5hmC was frequent in intragenic regions of up-regulated genes (10 genes), while the loss of 5hmC—in down-regulated genes (12 genes; Fig. 2d and Online Resource 3). Due to the small number of significantly deregulated genes with changes of 5mC/5hmC marks, these associations were not statistically significant. GO analysis showed that most of these 5mC/5hmC-regulated genes were related to regulation of cell proliferation, migration, and cellular biosynthetic process (Online Resource 2).

5mC and 5hmC marks of pluripotency loci

For locus-specific analysis of 5mC and 5hmC, the key pluripotency genes *POU5F1*, *NANOG*, and *SOX2* were selected. These loci are known as epigenetically regulated in ESCs and MSCs and are expressed in both types of the cells. In ADSCs, DNA methylation was detected in 5′ region of the *POU5F1* and *NANOG* genes, while the *SOX2* locus was unmethylated (Fig. 3a). No changes in methylation of these genes occurred during cell differentiation, except of variation in *NANOG* methylation observed in one cell line.

The presence of 5hmC in CCGG context in 5′ and intragenic regions of these loci was measured by 5hmC-qPCR. Some levels of 5hmC were identified in the *POU5F1* (9.45 ± 1.30 %), *NANOG* (9.33 ± 0.90 %), and *SOX2* (5.94 ± 0.88 %) loci. Intragenic sequences of the genes *POU5F1* and *SOX2* possessed higher amounts of 5hmC than 5′ regions (Fig. 3b). Upon osteogenic differentiation significant decrease of 5hmC was observed in the

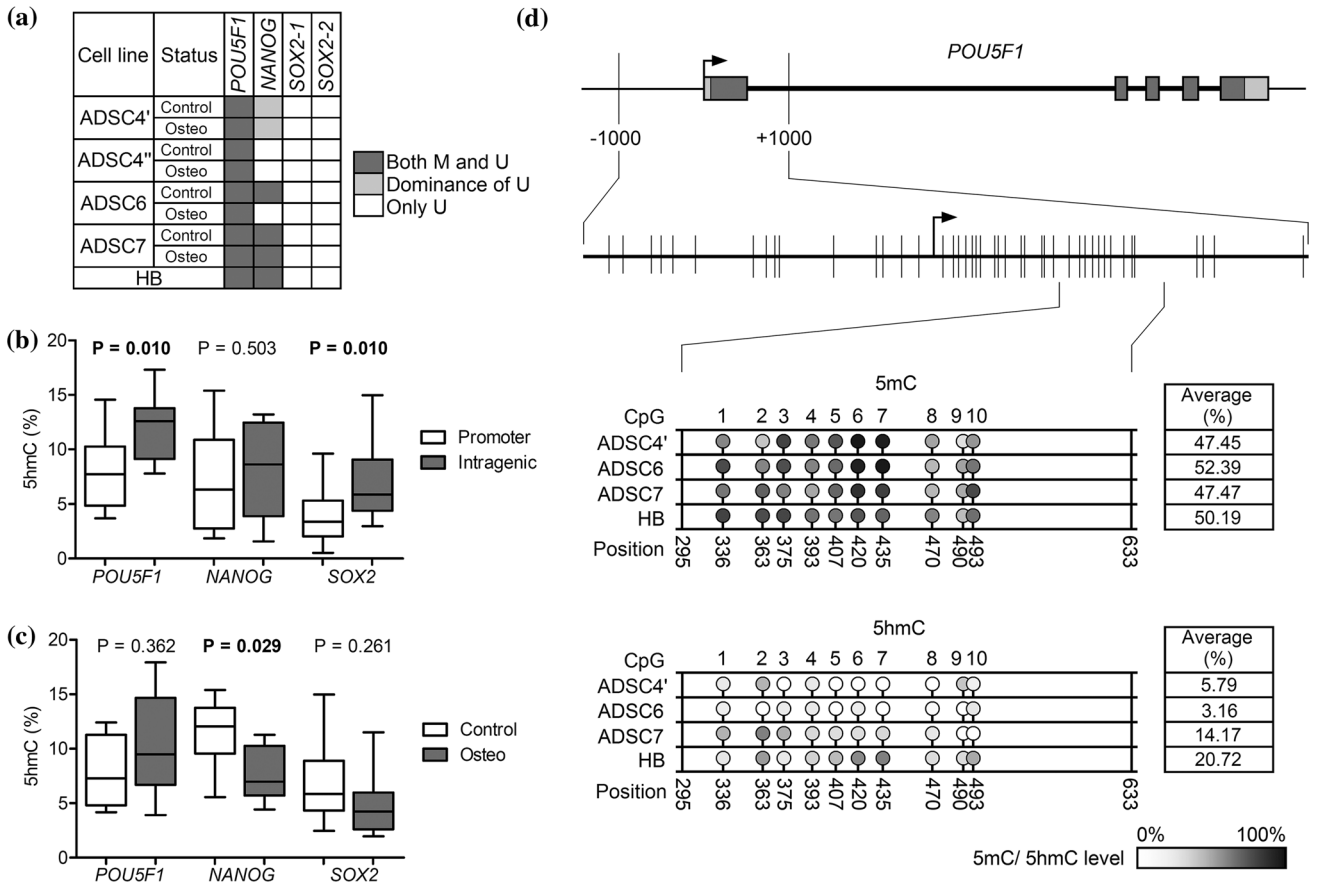

Fig. 3 5mC and 5hmC analysis of pluripotency genes in adipose-derived stem cells (ADSCs). **a** DNA methylation status in undifferentiated (Control) and osteogenically induced (Osteo) ADSCs and human brain (HB). Two fragments of the *SOX2* gene were analyzed. M—methylated sequence, U—unmethylated sequence. **b** 5hmC distribution according to the analyzed loci. **c** 5hmC distribution in undifferentiated (Control) and osteogenically induced (Osteo) ADSCs. **d** high throughput analysis of 5mC and 5hmC in a selected locus of *POU5F1*. *Arrow* shows transcription start site, darker and lighter boxes depict exons and untranslated regions, respectively. *Vertical crossing lines* represent all CpGs in the enlarged fragment

NANOG locus (Fig. 3c) that was in accordance with changes in the gene expression (Fig. 1d). As expected, the highest mean 5hmC level was detected in DNA from human brain tissue (24.21 ± 7.46 %) as compared to undifferentiated ADSCs (8.66 ± 0.94 %; $P = 0.002$).

For more precise quantification of 5mC and 5hmC at each CpG, a fragment covering 10 CpGs of the *POU5F1* gene, which showed the highest 5hmC level in undifferentiated ADSCs, was pyrosequenced with high throughput. A minimum coverage of 1538× (2395× on average) was obtained for all analyzed samples. Higher mean amount of 5hmC was observed in brain tissue as compared to ADSCs (20.72 ± 4.11 % and 7.70 ± 1.78 %, $P = 0.002$), while 5mC level of this region was almost equal in ADSCs and brain tissue (Fig. 3d). The most intense 5hmC accumulation was determined at CpG position #2 of both ADSCs and brain tissue. In contrast, positions #6 and #7 were enriched in 5mC in ADSCs and the levels (over 81 %) were higher than in brain tissue ($P = 0.029$ and $P = 0.048$). Cytosines at positions #8 and #9 were the least commonly modified bases in both ADSCs and brain tissue (Fig. 3d). When the levels of 5mC and 5hmC at each position were correlated with the gene expression, only the level of 5hmC at position #2 showed significant positive association ($P = 0.009$) with *POU5F1* expression in ADSCs.

Discussion

Accumulating data suggest significant involvement of the 5mC-to-5hmC conversion in various processes of cellular life that includes global changes in gene expression. In the present study, we performed a genome-wide profiling of 5hmC and 5mC marks in human adult stem cells and correlated them with the changes of gene expression occurring during the osteogenic differentiation. In overall, our study shows frequent changes in 5hmC profile and

increased expression of *TET1* during osteogenic differentiation of human ADSCs.

5hmC, first detected in mouse ESCs and cerebellar tissues [4, 18], was later identified in various human tissues [19]. In ESCs, 5hmC was shown as an important player in maintenance of cell pluripotency through activation of pluripotency-related genes expression [5, 20]. During cell differentiation, the pluripotency genes are mainly down-regulated, while the expression of tissue-specific genes increases. In agreement with this pattern, reduction of 5hmC and increase of 5mC levels were observed in pluripotency loci of differentiating cells [5, 20], while the gain of 5hmC was shown in differentiation-related loci [21]. Genome-wide analysis of 5hmC redistribution showed abundant changes in 5hmC profile during ESCs differentiation [7, 8]. The changes occurred in promoters, exons and enhancers, and differentiation-related genes acquired 5hmC in the gene body and were up-regulated [8]. Similarly to ESCs, dynamic changes of 5hmC were demonstrated during adult hematopoietic stem/progenitor cells differentiation to the erythroid lineage [22]. We analyzed genome-wide changes of 5mC and 5hmC profile during osteogenic differentiation of ADSCs and identified variation in location of both marks. Differently hydroxymethylated regions were 2.6 times more abundant than differently methylated regions, which is in a good agreement with the previous studies in ESCs [7, 8]. 5mC losses and 5hmC gains were the main events observed during ADSCs differentiation, and were accompanied by increased expression of *TET1*. Similarly, mouse Tet1, but not Tet2 or Tet3, were involved in maintenance of ESCs [5]. The comparison to gene expression pattern identified predominant gain of 5hmC in gene body of up-regulated genes, while inverse pattern was related to down-regulated gene expression, however, this association was not statistically significant. Predominant accumulation of 5hmC marks in the transcriptionally active loci, especially in gene bodies, was previously observed in ESCs and adult stem cells [8, 22, 23]. In overall, our data identified marked changes in epigenetic profile of differentiating ADSCs, and these changes involved variation in both 5mC and 5hmC marks. Only a small fraction of these epigenetic changes resulted in significant changes of gene expression, other processes impacted by this variation remains to be explored.

Cell differentiation potential depends on expression of the key pluripotency factors *POU5F1*, *NANOG*, and *SOX2*. Adult stem cells have more restricted differentiation potential than ESCs, and the expression levels of the pluripotency-related genes are relatively low [9]. However, in adult stem cells, the key regulators of cell plasticity *POU5F1* and *NANOG* have similar regulatory functions and target similar promoters like in ESCs [10, 11]. It was shown that, similarly to ESCs, decreased expression of *POU5F1* and *NANOG* can impair proliferative capacity and differentiation potential of MSCs, while overexpression of these factors protects MSCs from spontaneous differentiation during expansion in cell culture [10]. In ESCs, the promoters of these genes are epigenetically regulated. During ESCs differentiation, *POU5F1* and *NANOG* promoters have been shown to become repressed by DNA methylation [24, 25], while the *SOX2* promoter can be inactivated through trimethylation of H3K27 and H3K9 [25]. More recent studies [7, 26, 27] showed the presence of 5hmC in the *POU5F1* and *NANOG* loci in reprogrammed cells expressing these genes. In agreement with previous studies [28–30], which demonstrated in transcript and protein level the presence of the main pluripotency factors in ADSCs, we observed apparent levels of the *POU5F1* and *NANOG* transcripts, but quite low level of *SOX2* in our cell lines. Similarly to previously reported data [31], the promoters of *POU5F1* and *NANOG* were methylated in ADSCs. More detailed analysis revealed that at least a fraction of these cytosine modifications was composed of 5hmC marks, indistinguishable by bisulfite-based methods used in previous studies. In our study, the highest level of 5hmC was observed in the *POU5F1* gene that was consistently expressed in ADSCs. Moreover, as indicated by deep sequencing, hydroxymethylation of cytosine at specific location showed significant association to *POU5F1* expression levels.

MSCs are the multipotent adult stem cells of high importance for regenerative medicine. The therapeutic usage of MSCs depends on their differentiation potential which is epigenetically determined [9]. However, the knowledge of DNA modification profile of MSCs is mainly limited to the detection of DNA methylation profile of differentiated or senescent MSCs [32, 33]. Our study provides first data on genome-wide distribution of 5mC and 5hmC modifications in ADSCs and shows abundant changes in 5hmC profile during osteogenic differentiation of the cells. As a limitation, in our study, only cells of early passages were used and were collected from 3 mid-aged donors. Further attempts are needed to clarify the genome-wide 5hmC profile of MSCs in later passages. Recent study [13] showed significant reduction of overall 5hmC level, decreased production of *POU5F1* and *NANOG*, and impaired differentiation potential of ADSCs from aged donors. The osteogenic differentiation potential of these cells was improved by exposure to demethylating agent 5-azacytidine, but the mechanism remained obscure. Our study for the first time shows the presence of 5hmC in addition to 5mC in cell multipotency-related loci of ADSCs and suggests involvement of 5hmC in maintenance of low but consistent levels of *POU5F1*—the significant determinant of differentiation potential of adult stem cells.

Conclusion

Our study suggests the involvement of 5hmC in maintenance of small levels of the *POU5F1* transcript in ADSCs and indicates abundant changes in 5hmC profile during osteogenic differentiation of these adult stem cells.

Acknowledgments This study was funded by the Research Council of Lithuania (RCL) (Grant No. MIP 026/2012). Adipose tissue collection, stem cell isolation and cultures were also supported by EC FP7 Project "ADIPOA" (Grant No. HEALTH-F5-2010-241719). RM was supported by the Grant for Promotion of Student Scientific Activities (No. VP1-3.1-SMM-01-V-02-003) from RCL.

Compliance with ethical standards

Conflict of Interest The authors declare that they have no conflict of interest.

References

1. Mizuno H, Tobita M, Uysal C (2012) Concise review: adipose-derived stem cells as a novel tool for future regenerative medicine. Stem Cells 30:804–810. doi:10.1002/stem.1076
2. Uzbas F, May ID, Parisi AM, Thompson SK, Kaya A, Perkins AD, Memili E (2015) Molecular physiognomies and applications of adipose-derived stem cells. Stem Cell Rev 11:298–308. doi:10.1007/s12015-014-9578-0
3. Dent SY, Chen T (2014) Chromatin modifiers and remodellers: regulators of cellular differentiation. Nat Rev Genet 15:93–106. doi:10.1038/nrg3607
4. Tahiliani M, Koh KP, Shen Y, Pastor WA, Bandukwala H, Brudno Y, Agarwal S, Iyer LM, Liu DR, Aravind L, Rao A (2009) Conversion of 5-methylcytosine to 5-hydroxymethylcytosine in mammalian DNA by MLL partner TET1. Science 324:930–935. doi:10.1126/science.1170116
5. Ito S, D'Alessio AC, Taranova OV, Hong K, Sowers LC, Zhang Y (2010) Role of Tet proteins in 5mC to 5hmC conversion, ES-cell self-renewal and inner cell mass specification. Nature 466:1129–1133. doi:10.1038/nature09303
6. Zhao H, Chen T (2013) Tet family of 5-methylcytosine dioxygenases in mammalian development. J Hum Genet 58:421–427. doi:10.1038/jhg.2013.63
7. Gao Y, Chen J, Li K, Wu T, Huang B, Liu W, Kou X, Zhang Y, Huang H, Jiang Y, Yao C, Liu X, Lu Z, Xu Z, Kang L, Chen J, Wang H, Cai T, Gao S (2013) Replacement of Oct4 by Tet1 during iPSC induction reveals an important role of DNA methylation and hydroxymethylation in reprogramming. Cell Stem Cell 12:453–469. doi:10.1016/j.stem.2013.02.005
8. Kim M, Park YK, Kang TW, Lee SH, Rhee YH, Park JL, Kim HJ, Lee D, Lee D, Kim SY, Kim YS (2013) Dynamic changes in DNA methylation and hydroxymethylation when hES cells undergo differentiation toward a neuronal lineage. Hum Mol Genet 23:657–667. doi:10.1093/hmg/ddt453
9. Aranda P, Agirre X, Ballestar E, Andreu EJ, Román-Gómez J, Prieto I, Martín-Subero JI, Cigudosa JC, Siebert R, Esteller M, Prosper F (2009) Epigenetic signatures associated with different levels of differentiation potential in human stem cells. PLoS One 4:e7809. doi:10.1371/journal.pone.0007809
10. Tsai CC, Su PF, Huang YF, Yew TL, Hung SC (2012) Oct4 and Nanog directly regulate Dnmt1 to maintain self-renewal and undifferentiated state in mesenchymal stem cells. Mol Cell 47:169–182. doi:10.1016/j.molcel.2012.06.020
11. Greco SJ, Liu K, Rameshwar P (2007) Functional similarities among genes regulated by OCT4 in human mesenchymal and embryonic stem cells. Stem Cells 25:3143–3154. doi:10.1634/stemcells.2007-0351
12. Seeliger C, Culmes M, Schyschka L, Yan X, Damm G, Wang Z, Kleeff J, Thasler WE, Hengstler J, Stöckle U, Ehnert S, Nüssler AK (2009) Decrease of global methylation improves significantly hepatic differentiation of Ad-MSCs: possible future application for urea detoxification. Cell Transpl 22:119–131. doi:10.3727/096368912X638946
13. Yan X, Ehnert S, Culmes M, Bachmann A, Seeliger C, Schyschka L, Wang Z, Rahmanian-Schwarz A, Stöckle U, De Sousa PA, Pelisek J, Nussler AK (2014) 5-azacytidine improves the osteogenic differentiation potential of aged human adipose-derived mesenchymal stem cells by DNA demethylation. PLoS One 9:e90846. doi:10.1371/journal.pone.0090846
14. Zhang RP, Shao JZ, Xiang LX (2011) GADD45A protein plays an essential role in active DNA demethylation during terminal osteogenic differentiation of adipose-derived mesenchymal stem cells. J Biol Chem 286:41083–41094. doi:10.1074/jbc.M111.258715
15. Bura A, Planat-Benard V, Bourin P, Silvestre JS, Gross F, Grolleau JL, Saint-Lebese B, Peyrafitte JA, Fleury S, Gadelorge M, Taurand M, Dupuis-Coronas S, Leobon B, Casteilla L (2014) Phase I trial: the use of autologous cultured adipose-derived stroma/stem cells to treat patients with non-revascularizable critical limb ischemia. Cytotherapy 16:245–257. doi:10.1016/j.jcyt.2013.11.011
16. Unguryte A, Bernotiene E, Venalis A (2010) Human mesenchymal adipose stromal cells from mature adipocyte fraction. Cent Eur J Biol 5:47–58. doi:10.2478/s11535-009-0073-6
17. Daniunaite K, Jarmalaite S (2014) Gene expression profile of osteogenically differentiated human adipose-derived stem cells. Gene Expression Omnibus. http://www.ncbi.nlm.nih.gov/geo/query/acc.cgi?acc=GSE63754
18. Kriaucionis S, Heintz N (2009) The nuclear DNA base 5-hydroxymethylcytosine is present in Purkinje neurons and the brain. Science 324:929–930. doi:10.1126/science.1169786
19. Nestor CE, Ottaviano R, Reddington J, Sproul D, Reinhardt D, Dunican D, Katz E, Dixon JM, Harrison DJ, Meehan RR (2012) Tissue type is a major modifier of the 5-hydroxymethylcytosine content of human genes. Genome Res 22:467–477. doi:10.1101/gr.126417.111
20. Ficz G, Branco MR, Santos F, Krueger F, Hore TA, Marques CJ, Andrews S, Reik W (2011) Dynamic regulation of 5-hydroxymethylcytosine in mouse ES cells and during differentiation. Nature 473:398–402. doi:10.1038/nature10008
21. Bocker MT, Tuorto F, Raddatz G, Musch T, Yang FC, Xu M, Lyko F, Breiling A (2012) Hydroxylation of 5-methylcytosine by TET2 maintains the active state of the mammalian HOXA cluster. Nat Commun 3:818. doi:10.1038/ncomms1826
22. Madzo J, Liu H, Rodriguez A, Vasanthakumar A, Sundaravel S, Caces DB, Looney TJ, Zhang L, Lepore JB, Macrae T, Duszynski R, Shih AH, Song CX, Yu M, Yu Y, Grossman R, Raumann B, Verma A, He C, Levine RL, Lavelle D, Lahn BT, Wickrema A, Godley LA (2014) Hydroxymethylation at gene regulatory regions directs stem/early progenitor cell commitment during erythropoiesis. Cell Rep 6:231–244. doi:10.1016/j.celrep.2013.11.044
23. Szulwach KE, Li X, Li Y, Song CX, Han JW, Kim S, Namburi S, Hermetz K, Kim JJ, Rudd MK, Yoon YS, Ren B, He C, Jin P (2011) Integrating 5-hydroxymethylcytosine into the epigenomic landscape of human embryonic stem cells. PLoS Genet 7:e1002154. doi:10.1371/journal.pgen.1002154

24. Deb-Rinker P, Ly D, Jezierski A, Sikorska M, Walker PR (2005) Sequential DNA methylation of the Nanog and Oct-4 upstream regions in human NT2 cells during neuronal differentiation. J Biol Chem 280:6257–6260. doi:10.1074/jbc.C400479200
25. Hawkins RD, Hon GC, Lee LK, Ngo Q, Lister R, Pelizzola M, Edsall LE, Kuan S, Luu Y, Klugman S, Antosiewicz-Bourget J, Ye Z, Espinoza C, Agarwahl S, Shen L, Ruotti V, Wang W, Stewart R, Thomson JA, Ecker JR, Ren B (2010) Distinct epigenomic landscapes of pluripotent and lineage-committed human cells. Cell Stem Cell 6:479–491. doi:10.1016/j.stem.2010.03.018
26. Piccolo FM, Bagci H, Brown KE, Landeira D, Soza-Ried J, Feytout A, Mooijman D, Hajkova P, Leitch HG, Tada T, Kriaucionis S, Dawlaty MM, Jaenisch R, Merkenschlager M, Fisher AG (2013) Different roles for Tet1 and Tet2 proteins in reprogramming-mediated erasure of imprints induced by EGC fusion. Mol Cell 49:1023–1033. doi:10.1016/j.molcel.2013.01.032
27. Doege CA, Inoue K, Yamashita T, Rhee DB, Travis S, Fujita R, Guarnieri P, Bhagat G, Vanti WB, Shih A, Levine RL, Nik S, Chen EI, Abeliovich A (2012) Early-stage epigenetic modification during somatic cell reprogramming by Parp1 and Tet2. Nature 488:652–655. doi:10.1038/nature11333
28. Sachs PC, Francis MP, Zhao M, Brumelle J, Rao RR, Elmore LW, Holt SE (2012) Defining essential stem cell characteristics in adipose-derived stromal cells extracted from distinct anatomical sites. Cell Tissue Res 349:505–515. doi:10.1007/s00441-012-1423-7
29. Dudakovic A, Camilleri E, Riester SM, Lewallen EA, Kvasha S, Chen X, Radel DJ, Anderson JM, Nair AA, Evans JM, Krych AJ, Smith J, Deyle DR, Stein JL, Stein GS, Im HJ, Cool SM, Westendorf JJ, Kakar S, Dietz AB, van Wijnen AJ (2014) High-resolution molecular validation of self-renewal and spontaneous differentiation in clinical-grade adipose-tissue derived human mesenchymal stem cells. J Cell Biochem 115:1816–1828. doi:10.1002/jcb.24852
30. Riekstina U, Cakstina I, Parfejevs V, Hoogduijn M, Jankovskis G, Muiznieks I, Muceniece R, Ancans J (2009) Embryonic stem cell marker expression pattern in human mesenchymal stem cells derived from bone marrow, adipose tissue, heart and dermis. Stem Cell Rev 5:378–386. doi:10.1007/s12015-009-9094-9
31. Barrand S, Collas P (2010) Chromatin states of core pluripotency-associated genes in pluripotent, multipotent and differentiated cells. Biochem Biophys Res Commun 391:762–767. doi:10.1016/j.bbrc.2009.11.134
32. Berdasco M, Melguizo C, Prados J, Gómez A, Alaminos M, Pujana MA, Lopez M, Setien F, Ortiz R, Zafra I, Aranega A, Esteller M (2012) DNA methylation plasticity of human adipose-derived stem cells in lineage commitment. Am J Pathol 181:2079–2093. doi:10.1016/j.ajpath.2012.08.016
33. Schellenberg A, Stiehl T, Horn P, Joussen S, Pallua N, Ho AD, Wagner W (2012) Population dynamics of mesenchymal stromal cells during culture expansion. Cytotherapy 14:401–411. doi:10.3109/14653249.2011.640669